Adsorption study of Activated soot and its application as an adsorbent surface for removal of Alizarine Red S from aqueous Solution

Yasmine Salam Hassan[1,*], Hassan Sabeeh Jabr[1]

[1] *Department of Chemistry, College of Science, Al Muthanna University.*

[*] *Corresponding Author:* yasminesalam352@gmail.com

Received 16May2022, accepted 12June2022, published 31December2022.

DOI: 10.52113/2/09.02.2022/1-10

Abstract: In this study, activated soot (AS_2) has been produced using materials that are both affordable and available. The preparation of the AS_2 is done by thermal treatment of the soot at 400℃ for 2 hours. XRD, SEM, and FTIR techniques were used to characterize the properties of the prepared AS_2. The AS_2 was used for Alizarine Red S (AR) dye adsorption from aqueous solutions. Several experimental parameters have been tested to study the properties of AS_2 as an adsorbent, which include temperature, adsorbent weight, time, and the influence of pH. The results indicate that the AS_2 has good adsorbent properties. Moreover, other remarks have been found such as the adsorption efficiency increased at pH=4 and decreased at pH=10. The rise in temperature has a negative impact on the adsorption efficiency. Finally, the optimal adsorbent weight was found to be 0.08 g and the optimal contact time was 15 min.

Keywords: Activated soot (AS2), soot (AS1), Adsorption, Alizarine Red S (AR).

1. Introduction

The causes of health problems and their costs are of urgent concern to scholars and governments around the world. Environmental pollution, such as air pollution, is the most important factor to be discussed. Air pollution is a deep cause of soaring health costs. The harm caused by air pollution to the health of residents has been proven, such as in the Great Smog in London in 1952, which shocked the world by killing tens of thousands of people. A large amount of energy consumption and the development of urbanization under the invention of the steam engine by Watt in the UK and the booming industrial revolution made air pollution more and more serious, and caused damage to human health. Therefore, a large amount of literature on the relationship between air pollution and health was released, such as the effect of air pollutantconcentration on the

© Hassan, 2022. This is an open-access article distributed under the terms of the Creative Commons Attribution 4.0 International license

mortality and morbidity of different populations [1].

With the quick growth and development of agriculture and industry, the quality of life has improved, thereby requiring a higher standard of environmental ecosystem and daily supply. However, large amounts of various pollutants such as metal ions, persistent organic pollutants (POPs), antibiotics, cosmetics, dyes and others are inevitably released into the natural environment such as soils, water, rivers, and lakes. The pollutants in soils, lakes, rivers and groundwater could be accumulated and at last enter the human body through the food chain. Thereby, the efficient elimination of pollutants from aqueous solutions is crucial for environmental protection and human health. Although different kinds of techniques such as coprecipitation, membrane, adsorption, oxidation–reduction, degradation, ion exchange, transformation and others have been applied to remove the pollutants from large volume of solutions or in-situ solidifaction/immobilization on solid phases, it is still a worldwide challenge for the efficient decontamination of pollutants from solid phases such as soils and sediments, especially at low concentrations. The photocatalytic degradation of POPs or reduction of metal ions is one effective strategy for in-situ decontamination to reduce the organic contaminant concentration or immobilize the heavy metal ions on solid particles [2].

This research was aimed to assess the effectiveness of activated carbon in dye adsorption from aqueous solutions, where particles of soot as Adsorbent substance was used and the factors effecting the adsorption process such as: pH, contact time, absorbent weight, temperature were determined.

2. Experimental Procedure

2.1 The materials

The chemicals in this research were purchased from the companies Sigma Aldrich and BDH.

The Hummer's solution contains 36% HCl, 98% NaOH, 98% $NaNO_3$, 97% $KMnO_4$, and 98% H_2SO4.

62.2. The Instruments

The FTIR spectrum has a range of (400-4000) cm^{-1} and was obtained from a Shimadzu FT-IR-8000 Fourier transform infrared spectrophotometer. Furthermore, the XRD analysis is carried out on the D6000 x-ray diffractometer equipment. The diffraction intensity of Cu Ka radiation produced at 40 Kv was measured in the range of 2Ɵ to 80.

A scanning electron microscope (SEM) with the model number FEI Nova Nano SEM 450 was used to analyze the surface morphology of activated carbon. The accelerating voltage is set between 15-20 kilovolts. The AS2's surface morphology photos were taken at various magnification levels. The specific surface area (BET) and porosity were also measured using the ASAP 2460.

2.3 Preparation of Activated carbon from the soot

The soot was prepared from candle paraffine and collected in clean and dry beaker. The cleaned soot was dried for 24 hr in an oven set to 80 ºC. Thereafter, the dried soot was grinded and sieved to a particle size of 125 μm to obtain activated carbon.

2.4 Preparation of standard solution of alizarine red S

The maximum absorbance wavelength (λmax) of Alizarine Red S dye was determined using an absorbance spectrum ranged from (200-800 nm) by the UV-Visible spectrophotometer, and the stock solution (100 ppm) of Alizarine Red S dye was prepared by dissolving (0.25g) of Alizarine Red S dye in 500 ml of distilled water. A calibration curve was created by preparing a series of dye solutions at various concentrations (0.3-100 ppm).

The chemical structures of Alizarine Red S dye are shown in Figure 1.

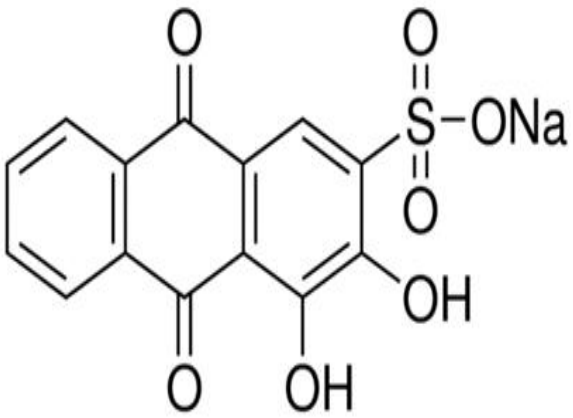

Fig. (1): Chemical structure of Alizarine Red S dye.

2.5. Study factors affecting on the adsorption process

2.5.1. Study the effect of an Equilibrium time of Adsorption

For determining the equilibrium time between the adsorbed quantity of dye and the adsorbent, the dye concentration 100 ppm was selected at different times (5, 10, 15, 20, 25, 30 and 60 min). at constant temperature 25 ºC and constant volume of dye solution (25 ml) and using a constant weight of the activated carbon (0.08 g) and the pH of the dye solutions was not changed, the test tubes were placed in the water bath with shaker at a speed 180 rpm, after that the solution was separated in a centrifuge for 20 min. Then the absorbance of dye solution was measured at 515 and 536 nm.

2.5.2. Study the influence of the pH on adsorption

Effect of the pH on the adsorption process. The dye concentration 100 ppm was selected and constant volume of dye solution at different pH values (4, 7, and 10), adjustments were made using 1M HCl or NaOH solution, the temperature was 25 °C and using the constant weight of absorbent 0.08g and equilibrium time 15 min. the test tubes were placed in the water bath with a shaker at a speed 180 rpm then the solution was separated in a centrifuge for 20

minutes then the absorbance of dye solution was measured at 515 and 536 nm.

2.5.3. Study the influence of the temperature on

The
con
of a
diff
min
min
2.5.
Five
0.02
the
thea
volu
time
taken. The test tubes were placed in the water bath with shaker at a speed 180 rpm. The solutions were placed in a centrifuge for 15 min, then the absorbance of the dye solutions was measured at 515 and 536 nm.

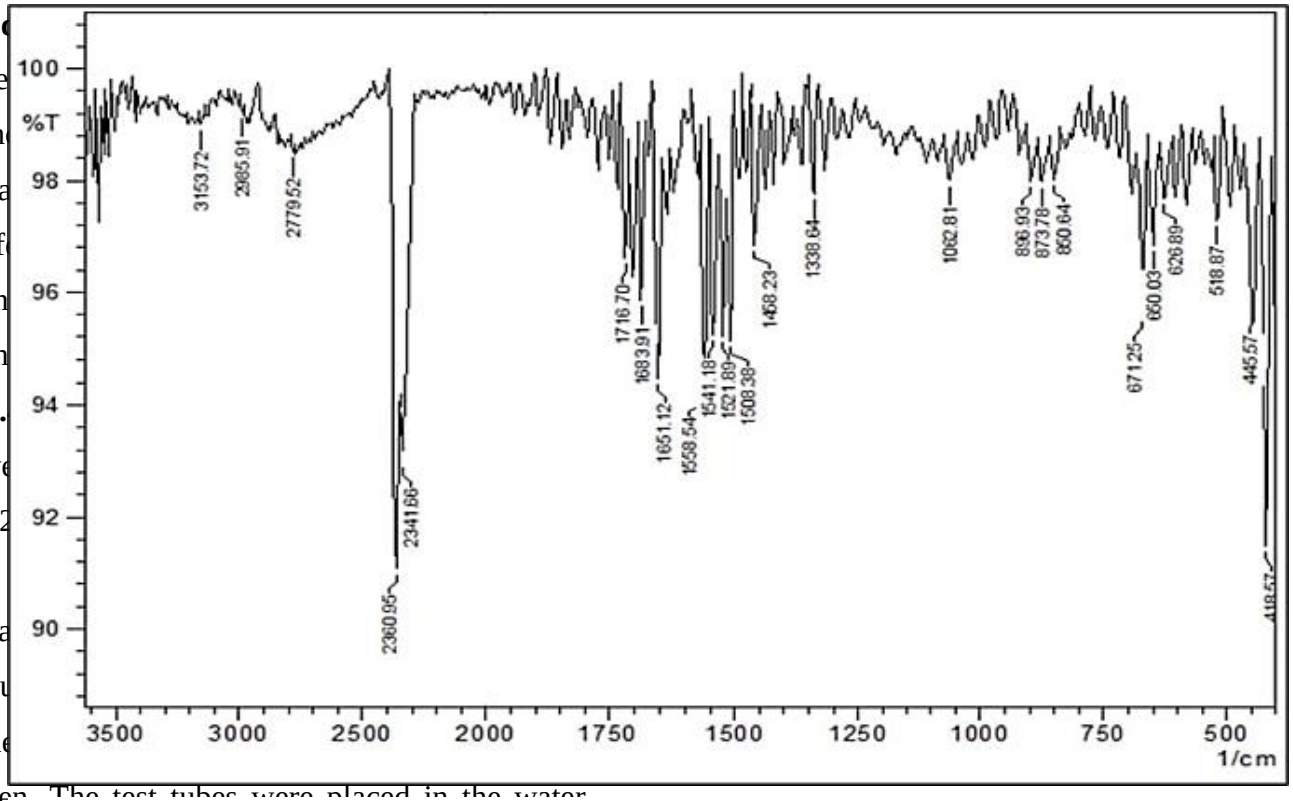

Fig. (2): The FT-IR Spectrum of AS2.

2.6. Batch adsorption experiments

The influence of several parameters for ARS adsorption, such as the initial ARS concentration 10-50 mg/L, pH value (3.0–11.0), contact time (0–30 min), and temperature (25–45 °C), were examined to establish optimal adsorption conditions. All batch adsorption studies were carried out with a dye solution of 25 ml. Each experiment was carried out in a thermostatic shaker with a 180 rpm shaking rate. All of the adsorption experiments were done three times. The following formula was used to compute the adsorption quantity (Q) of ARS:

$$\ln q_e - q_t = \ln q_e - K_1\, t \qquad (3)$$

Where Qe and Qt are the adsorption quantities of ARS absorbed at equilibrium and at any time (mg.g-1), respectively, and K1 (1/min) is the pseudo-first-order adsorption rate constant. The slope and intercept of the plot of ln (qe-qt) vs time t (min) yielded the values of K1 and qe, respectively. The pseudo-second-order model is as follows:

$$\frac{\mathrm{t}}{q_t} = \frac{1}{\mathrm{k2} * \mathrm{q}_e^2} + \frac{1}{q_e} * \mathrm{t} \qquad (4)$$

The slopes and intercepts of plots of t/qt vs t (min) were used to compute the second-order

rate constant K2 and qe, while K2 (g/mg min) reflects the rate constant of the pseudo-second order model. ARS concentration was measured using an a UV–visible spectrophotometer.

3. Results and Discussion

3.1 Characterization of AS2 surface

The FT-IR spectrum of AS2 (figure 2) revealed the existence of absorption bands (O-H) at 3153 cm^{-1}, strong bands (-CH) at 2985 cm^{-1}, and 1558 cm^{-1} for the C=O and C=C groups, respectively. Finally, the bending of the C-H group showed bands at 1427.37 and 1377.22 cm^{-1}. [15].

X-ray diffraction (XRD) technology was used to characterize the amorphous structure of the prepared surface (AS2), the spectrum (intensity versus 2θ) is displayed in figure 3.

At 325o, the band at 2θ= 29.00 reverts to AS2's non-crystalline form.

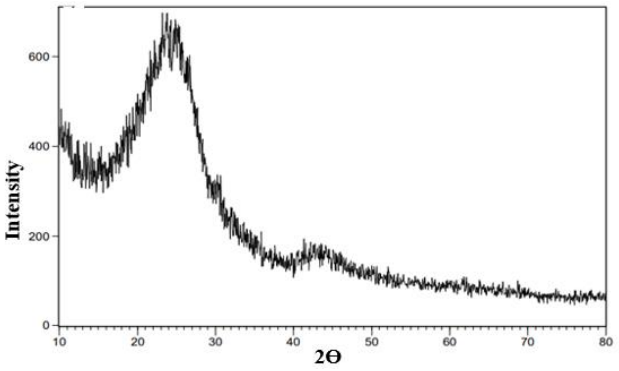

Fig. (3): The X-ray diffraction pattern for AS2.

The surface morphology of AS1 before and after activation is shown in SEM. Spherical regular particles were visible before activation of AS1. There were two distinct particles visible: bright and black. The particle size was calculated to be 50 nm.

The soot AS2 morphology showed two different types of particles after activation. The light ones were grouped together, while the dark ones were randomly scattered around the surface. The size of all particles was uniform [16].

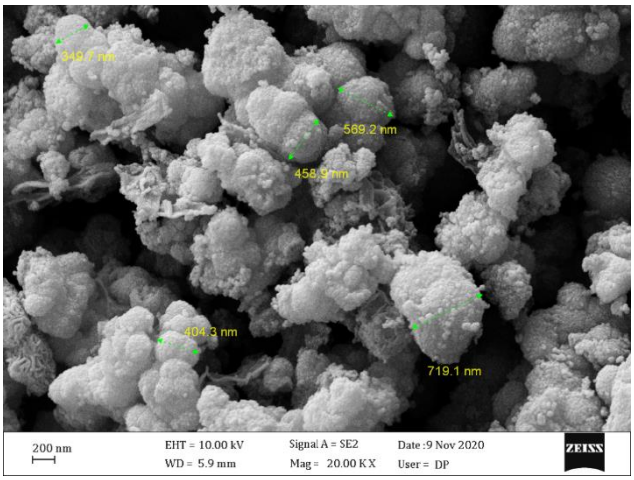

Fig. (4): The SEM of AS1.

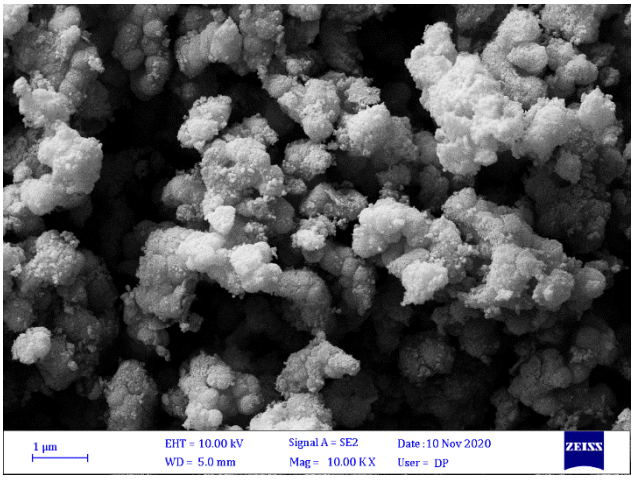

Fig. (5): The SEM of AS2.

The surface area of the activated soot AS2 treated with Hummer's solution increased to be 93.931 m^2g^{-1} when compared to AS1. This could be due to the agglomeration of carbon granules caused by the formation of positively and negatively charged active atoms on the surface and the attraction between them, causing a shrinkage in the carbon surface and a decrease

in the surface area. This conforms the SEM examination of the AS2 surface, which revealed conglomerates [17]. AS1 had a total pore diameter of 13.857 nm, while AS2 had a total pore diameter of 20.797 nm. Figure 6 shows that the hysteresis loop of AS1& AS2 is connected to capillary condensation and ranged from 0.25 P/Po 0.5. According to the IUPAC classification, this isotherm is belonging to the type III.

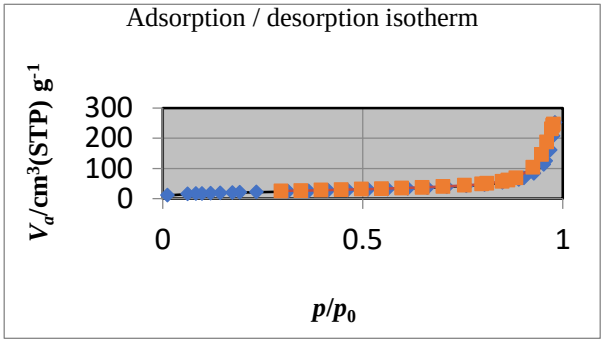

Fig. (3): The (N2) adsorption-desorption isotherms of AS2.

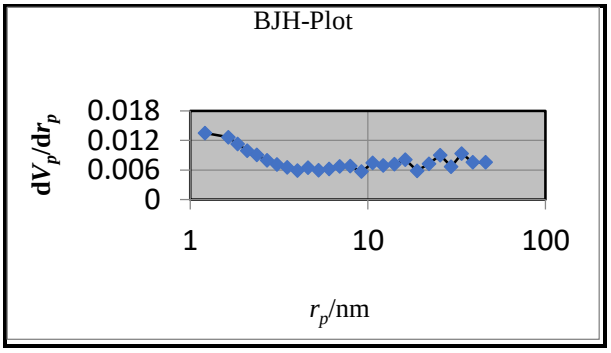

Fig. (4): corresponding pore size distribution of AS2.

3.2 Thermodynamics of adsorption process

Adsorption processes were studied using thermodynamics to determine the nature of the adsorption response. Thermodynamic characteristics at 298 to 318 K of adsorption include entropy (S°), Gibbs free energy (G°), and change in standard enthalpy (H°), which are all crucial to examine. The following equation [18] can be used to determine Gibbs free energy change:

$$\Delta G^{\circ} = -RT \ln k_e$$

G° represents the Gibbs free energy change (KJ.mol^{-1}), R represents the universal gas constant (8.314 J.mol^{-1}.K^{-1}), T represents the absolute solution temperature (in Kelvin), and k_e represents the thermodynamic equilibrium constant for adsorption. As a result, the value of (k) has been estimated using the equation [19]:

$$k_e = \frac{q_e m}{C_e V}$$

Where, the change in standard enthalpy (ΔH°) has been calculated by plotting the values of lnk against 1/T according to Van't Hoff-Arrhenius equation [17]:

$$\text{Ln } k_e = \frac{\Delta S^{\circ}}{R} - \frac{\Delta H^{\circ}}{RT}$$

The values of ((ΔS°)/R) and (ΔH°)/RT) have been calculated from the intercept and slope of the linear plots [20] the data that illustrated in Table 1 were obtained from the intercept and slope,.

Table 1: Values of the equilibrium constant (ke) and thermodynamic parameters of adsorption the AR dye onto AS2.

T(C°)	25	35	45
T(K)	298	308	318
1/T (K-1)	0.0033	0.0032	0.0031
Ke	2.515	1.979	1.585

Ln Ke	2.515	1.979	1.585
-Δ*G*° (J.mol^{-1})	2284.997	1747.921	1217.717
-Δ*H*° (KJ.mol^{-1})		18.19	
Δ***S***°(J.mol^{-1} .K^{-1})		75.95	

3.3 Adsorption isotherms

The linear versions of the Freundlich and Langmuir model isotherms, described by the equations below, were used to analyze the experimental results. Isotherm of friendship;

$$logq_e = logK_f + \frac{1}{n}\, logC_e$$

Where qe represents the quantity of adsorbed at equilibrium in mg.g-1, Ce represents the concentration at equilibrium in mg L^{-1}, Kf represents the adsorption capacity, and n represents the intensity of adsorption. When you plot log qe against log Ce, you get a slope of (1/n) and an intercept of log kf. In addition, the Langmuir isotherm equals:

$$\frac{C_e}{q_e} = \frac{1}{b\, K_L} + \frac{C_e}{K_L}$$

Where K is the Langmuir constant related to adsorption capacity mgg^{-1}, and Lmg^{-1} is the Langmuir constant related to adsorption intensity. The sorption of AR on AS2 was studied utilizing Freundlich and Langmuir adsorption isotherms using straight line equations for assessed adsorption isotherm constants. The plot of (Ce/qe) against Ce yields a straight line with a slope of (1/KL) and an intercept of (1/bkL). The parameters of adsorption isotherms were obtained and listed in tables (2 and 3). The results revealed that the adsorption of AR dyes on AS2 matched the Freundlich model. These findings confirm that AR dye adsorption on AS2 is a physical adsorption caused by the formation of a multilayer on the AS2 surface that is strongly conducted to the dye molecules [21].

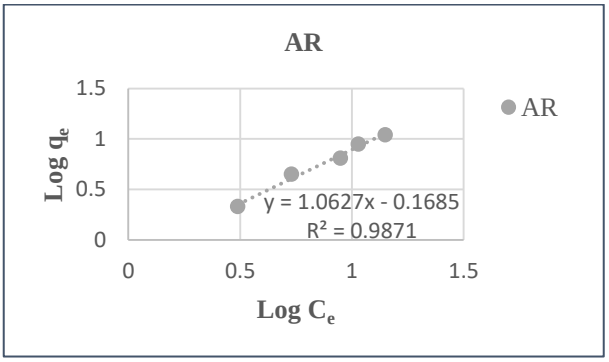

Fig. (5): The linear of Freundlich equation of three dyes for AS2.

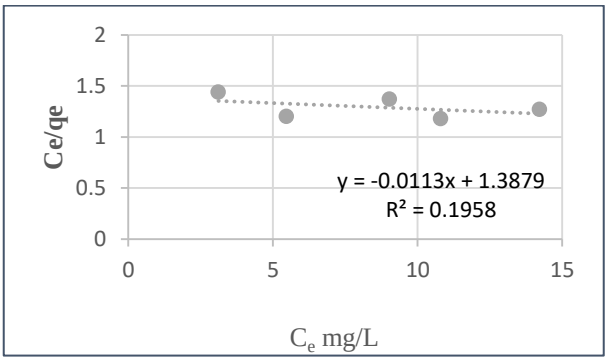

Fig. (6): The linear of Langmuir equation of three dyes for AS2.

Table 2: Values of the parameters of freundlich equation for AR into AS2.

Freundlich constants

Kf (mg/g)	0.678
n (L/mg)	0.94
R^2	0.987

Table 3: Values of the parameters of Langmuir equation for AR into AS2.

Langmuir constants	
K_L (mg/g)	88.49
b (L/mg)	0.008
R^2	0.195

3.4 study of kinetic properties

The adsorption kinetic study is critical for determining the efficiency and mechanism of adsorption since it describes the rate of solute uptake at the solid-solution interface as well as any rate-control mechanisms. The adsorption kinetic of AR on the surface of AS2 adsorbent was investigated in this study. The Lagergren pseudo—first—order and pseudo—second—order models [22] were used to analyze the adsorption kinetics of AR onto AS2 adsorbent. For the adsorption of a solute from a liquid solution, the Lagergren rate equation is one of the most extensively used adsorption rate equations. The following equation can be used to express the pseudo–first–order kinetic model (Eq.3).

$$\ln(q_e - q_t) = lnq_e - k1 * t$$

where qt represents the amount of dye adsorbed in mgg^{-1} at time (t), qe represents the maximal adsorption capacity, and k represents the first-order rate constant in ($min.^{-1}$). For the adsorption of AR on AS2, the plot versus time (t) produces a slope of (-k1/2.303) and an intercept of (log qe) to estimate the adsorption capacity and adsorption rate constants, as illustrated in Fig. 7. The second–order kinetics of adsorption were investigated using the Largerger equation [23].

$$\frac{t}{q_t} = \frac{1}{k2 * q_e^2} + \frac{1}{q_e} * t \qquad (5)$$

K2 is the second-order rate constant in $mg.g^{-1}.min^{-1}$, and qe is the equilibrium adsorption capacity in mg/g. When (t/qt) is plotted against time (t) to estimate the adsorption capacity and adsorption rate constants, the values of qe and k2 are obtained, as shown in Figure 10, from the slope and intercept, respectively. The best correlation for the system provided by the pseudo-first order model from the start of adsorption up to 15 minutes may be attributed to more vacant sites on the surface of the adsorbent and the high concentration of adsorbate, according to the kinetic adsorption of both dyes. According to the correlation factors, the results were best suited to a pseudo second order kinetic after 15 minutes, which could be attributable to the occupation of all sites on the adsorbent surface and reaching adsorption equilibrium. Table 4 shows the kinetics parameters results.

Table 4: Kinetic parameters for sorption of Alizarin Red S (AR) on AS2 adsorbents.

1st order		
qe (cal) (mg/gm)	K1 1/min	R2
13.19	0.023	0.349
2nd order		
qe(cal) (mg/gm)	K2 min-1.gm.mg-	R2
1.06	-0.034	0.949

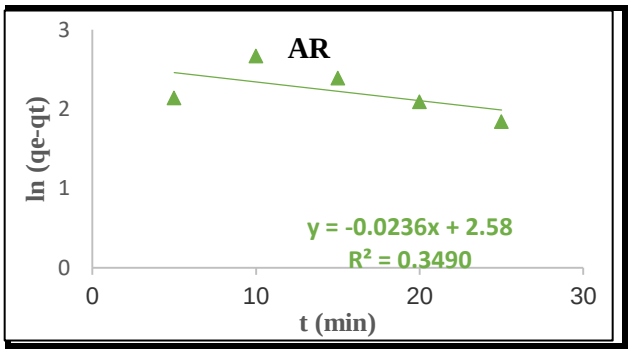

Fig. (7): The Pseudo first order kinetics of the ARS dyes onto AS2.

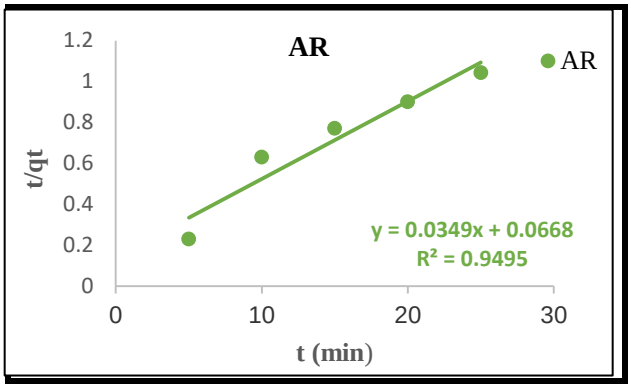

Fig. (8): The Pseudo second order kinetics of the three dyes onto AS2.

4. Conclusions

In this study, we found that: the chemical activation with sulphuric acid can create efficient activated carbon at a reasonable cost. The soot was treated with Hummer's solution to be activated. The pH 4 was the ideal for excellent AR dye adsorption. The results showed that the percentage of dye removed increases as the adsorbent weight increases. The finding of the thermodynamic study is that AR dye adsorption on soot and activated soot was exothermic and spontaneous, as determined from DH and DG.

References

[1] Xiaocang, X., Yang, H., Li, C., Theoretical model and actual characteristics of air pollution affecting health cost: a review, International Journal of Environmental Research and Public Health 19.6 (2022): 3532.

[2] Lu, Yin, et al. "Application of biochar-based photocatalysts for adsorption-(photo) degradation/reduction of environmental contaminants: mechanism, challenges and perspective." Biochar 4.1 (2022): 1-24.

[3] Z. M. Lazim and T. Hadibarata, “Adsorption Characteristics of Bisphenol A onto Low-Cost Modified Phyto- Waste Material in Aqueous Solution Adsorption Characteristics of Bisphenol A onto Low-Cost Modified Phyto-Waste Material in Aqueous Solution,” Water, Air, & Soil Pollution, vol. 226, no. 3, pp.1-11, 2015.

[4] A. S. Waheeb, H. Abbas, H. Alshamsi, M. K. Al-hussainawy, and H. R. Saud, “Myristica fragrans Shells as Potential Low Cost Bio-

Adsorbent for the Efficient Removal of Rose Bengal from Aqueous Solution : Characteristic and Kinetic Study," Indonesian Journal of Chemistry.[

[5] A. M. Alasadi, F. I. Khaili, and A. M. Awwad, "Adsorption of Cu (II), Ni (II) and Zn (II) ions by nano kaolinite : Thermodynamics and kinetics studies," pp. 258–268, 2019.

[6] A. M. Alasadi, F. I. Khaili, and A. M. Awwad, "Adsorption of Cu (II), Ni (II) and Zn (II) ions by nano kaolinite : Thermodynamics and kinetics studies," pp. 258–268, 2019.

[7] W. A. M. Mcminn and T. R. A. Magee, "Water sorption isotherms of starch powders Part 1 : mathematical description of experimental data," Journal of food Engineering, vol. 61, no.3, pp. 297–307, 2004.

[8] B. S. Journal, "Adsorption of Congo, Red Rhodamine B and Disperse Blue Dyes From Aqueous Solution onto Raw Flint Clay," Baghdad Sci. J., vol. 9, no. 4, pp. 680–688, 2012

[9] [B. K. Nandi, A. Goswami and M. K. Purkait, "Adsorption characteristics of brilliant green dye on kaolin," Journal of hazardous materials., vol. 161, no. 1, pp. 387-395, 2009.].102] B. S. Journal, "Adsorption of Congo, Red Rhodamine B and Disperse Blue Dyes From Aqueous Solution onto Raw Flint Clay," Baghdad Sci. J., vol. 9, no. 4, pp. 680–688, 2012

[10] [B. K. Nandi, A. Goswami and M. K. Purkait, "Adsorption characteristics of brilliant green dye on kaolin," Journal of hazardous materials., vol. 161, no. 1, pp. 387-395, 2009.].vol. 20, no. 5, pp. 1152–1162, 2020.

[11] Vidyadhar V G, Pranay R, Anup Ch and Pranav P 2019 Kinetic, Thermodynamics and Equilibrium Studies on the Removal of Congo Red Dye using Activated Teak Leaf Powder (Applied Water Science) pp 9–55.